EFFECT OF CERAMIC FOAM FILTERS ON OXIDES REMOVAL AND THE TENSILE PROPERTIES OF A-356 ALLOY CASTINGS

A. Khakzadshahandashti[1], N.Varahram[2] and P. Davami[2]

* *a.khackzad@gmail.com*

Received: september 2013 **Accepted: March 2014**

1 Department of Engineering Ayatollah Amoli Branch, Islamic Azad University, Amol, Iran.

2 Devision of Casting Department of Materials Science and Engineering, Sharif University of Technology, Tehran, Iran.

Abstract: *This article examines the Weibull statistical analysis that was used for investigating the effect of melt filtration on tensile properties and defects formed inside the casting. Forming and entrapping of double oxide films have been explained by using the context of critical velocity of melt in the runner. SutCast software results were used to examine the amounts of the velocity of melt as such. SEM/EDX analysis is used to observe the presence of double oxide films in the fracture surfaces of the tensile specimens. The article goes on to propose that castings made with foam filters with smaller pores show higher mechanical properties and reliability due to higher Weibull modulus and fewer defects.*

Keywords: *Double oxide film defect, Ceramic foam filter, Weibull module, Aluminum A356 alloy, Critical velocity*

1. INTRODUCTION

Al-Si-Mg alloys have wide spread usage in the automotive and aerospace industries, compared to other aluminum alloys, as they show a good capability of casting, mechanical properties, corrosion resistance, weldability and low thermal expansion [1-4]. Various defects content such as pores and double oxide films are factors that play a major role in creating a great amount of variations of tensile properties in A356 castings [2,5,6]. Liu and Samuel [7] stated the importance of the effect of casting variables changes, as they affect defects content in the casting for designers due to the effect of defects on unexpected failure during the tensile tension. Since the elimination of complete defects seemed to be impossible, using proper casting method for obtaining a clean casting with minimum defects would be necessary for consistent mechanical properties [8].

Campbell [9] divided A356 casting defects into three groups of (i) gas porosities caused by entrapped gas in the melt, (ii) shrinkage porosities caused by volume reduction during solidification and (iii) oxide films from oxide particles entrapped at the solidification zone. Unsuitable designing of the running system causes high and undesirable melt velocity, and this leads to turbulence of melt surface, so the oxide layer at the melt surface folds and is entrapped in the melt [2]. The oxide layer at the melt surface acts as a melt preservative from further oxidation and gas diffusion to the melt beneath, so the disadvantages of oxide films start when they sink into the melt. This folded layer entraps the little amount of gas. Clearly one side of oxide film in contact with the melt is in a strong atomic contact, but the other side is in contact with air (a mixture of Nitrogen, Hydrogen, Oxygen and Argon). This interface between two oxide layers separated by the remaining atmosphere is a vulnerable region in the casting during the tension test to form a crack, and these defects are known as the double oxide film [10,11]. Some researchers investigated the melt velocity which is the reason for surface turbulence during the casting process [12,13]. Campbell [14] reported that controlling the velocity at the range of 350 mm/s to 500 mm/s is necessary to eliminate the defects content in the casting. Most of these oxide films are accompanied by other casting defects such as pores, cracks and slags. Caceres and Selling [15] showed that reduction of tensile properties of Al-Si-Mg alloys is proportional with area percentage of inclusions and oxide films on the fracture surface. Convoluted oxide films can play the role of cracks in the casting, and these oxide films can affect mechanical properties consistently in a great extent [2]. Ardekhani and Raiszadeh [4]

explained the relation of the crack initiation and inclusions in their fractogtaphic observations. In many cases, the great amount of porosity accompanied by oxide films degrades tensile properties.

Showman [16] used ceramic foam filters as a part of the running system to reduce oxide inclusions and obtain higher tensile properties. Investigations reveal two positive effects of using ceramic foam filters in the running system. The first one is reducing the amount of inclusions in the casting by trapping them and preventing them from entering the mold cavity. The second positive effect of using filters is their ability to control the melt flow and prevent the melt turbulence, so the melt reoxidation after passing through the filter diminishes. Habibollah Zadeh and Campbell [17] measured the decrease of aluminum-silicon and cast iron melt velocity by 75 to 80 percent as they passed through a 20 ppi (pores per linear inch) ceramic foam filter. Hashemi and Raiszadeh [18] reported this reduction by 50 percent in Al-Si alloys.

This study examined the effect of using different ceramic foam filters in the A356 casting runner on the removal of double oxide films by using the Weibull statistical analysis. We also examined the influence of these changes on Weibull modulus and tensile properties.

2. EXPERIMENTAL PROCEDURE

What is used here is the A356 aluminum alloy with chemical composition that is determined by Optical Emission Spectroscopy (OES) shown in Table 1. The schematic sketch of the step mould castings implemented in this experiment is shown in Fig. 1. The actual dimensions of the aforementioned model and running system are given in Fig. 2 and Table 2, respectively. To study the effect of melt filtration, different ceramic foam filters were used. In other words, three types of moulds were used with different ceramic foam filters in the runner, one without using any filter and two with using 10 and 20 ppi ceramic foam filters in the runner. Therefore the only

Table 1. Exact chemical composition of the experimented alloy.

Si	Mg	Fe	Ti	Cu	Ni	Zn	Sn	Mn	Al
7.25	0.44	0.43	0.01	0.14	0.005	0.04	<0.005	0.02	Balance

Table 2. Dimensions of the running system components shown in Fig. 1 (all in mm).

Component	**Mould without filter**	**Mould with filter**
pouring basin	80×90 (depth 40)	80×90 (depth 40)
Top sprue cross section	Ø= 51	Ø= 51
Bottom sprue cross section	Ø= 40	Ø= 40
Sprue height	109.4	109.4
Filter size	…	15×18.1×40
Runner cross section	24.4×18.1	24.4×18.1

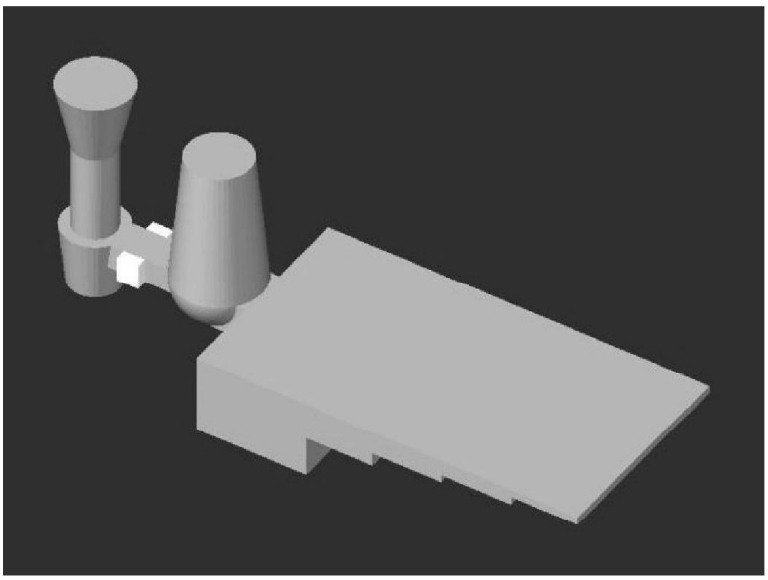

Fig. 1. Schematic sketch of the mould used in the experiment.

difference between these three cases was the various ceramic foam filter. The moulds were made by a CO_2 – silica sand mold processing. The A356 alloy used for each experiment was prepared in an electrical resistance furnace. The melt was degassed in a crucible by an Argon degassing ceramic lance for 300 seconds. 0.03 wt. % strontium was used for the microstructural modification. During these experiments, the degassing process, the modifier content, the pouring temperature, the chemical composition of the alloy and the casting time that affect the defects content in the casting were all kept constant, to examine the results of the above mentioned experiments and find the effect of melt filtration on double oxide films removal.

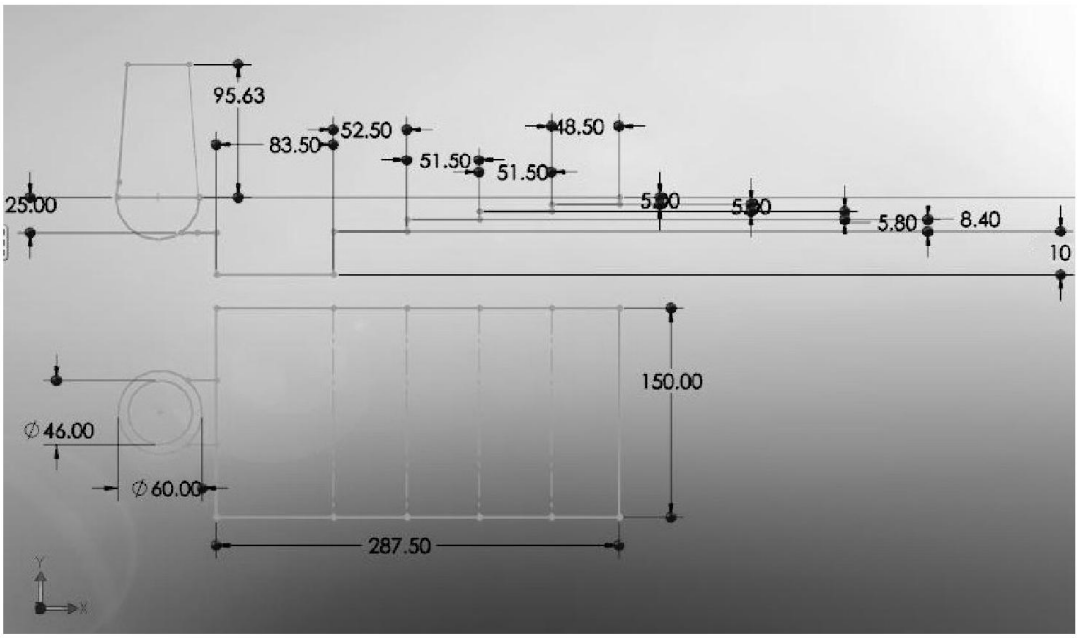

Fig. 2. The actual dimensions of the model shown in the Fig. 1 (all in mm).

The casting process for each mould was repeated for the second time to obtain more reliable results. After melting and degassing, the moulds were cast at the casting temperature of 720 .

Each mould had five sections with different thicknesses. Tensile test bars from four sections of each mould were studied, and results of eight specimens for two trials were studied. Tensile test bars were machined according to ASTM B557 to acquire dimensions of 25.4 mm gauge length, 6.35 mm thickness and 100 mm overall length. The thickness of all tensile test specimens was of the same value of 6.35 mm. Tensile test was done with a SANTAM STM-150 machine under a strain rate of 3.9×10^{-4}. TS and %EL results reported in this study were the average of minimum 4 similar trials.

Tiryakioğlu [19] explained a method for investigating the casting reliability. The value of P_f is the failure possibility of a casting in the tension of σ. In other words, it was the percentage of specimens which has failed in this tension. This value was calculated by using Eq. 1, in which σ_0 is the tension which 62.8% of specimens fail, and M is the Weibull modulus.

$$P_f = 1 - \mathrm{Exp}[-(\frac{\sigma}{\sigma_0})^M] \quad (1)$$

M is also obtained from Eq 2.

$$\mathrm{Ln}[\mathrm{Ln}(\frac{1}{1-P_f})] = M\mathrm{Ln}\sigma - M\mathrm{Ln}\sigma_0 \quad (2)$$

The value of M which is the slope of line fitted in the above equation was used to evaluate the scattering of tensile test results. Using the Weibull analysis is an effective approach for investigating the reliability of the casting. The higher Weibull modulus is the proof of higher results and properties, lower defects content and greater casting reliability. The value of P_f for the maximum value of σ is equal to 1, so the maximum value of TS and %El should not be considered in the Weibull analysis because of the term $\mathrm{Ln}[\mathrm{Ln}(\frac{1}{1-P_f})]$ in Eq. 2.

Drouzy [20] proposed the following empirical equation for calculating the quality index value.

$$Q_i = TS + d\log(s_f) \quad (3)$$

In Eq. 3, TS is the tensile strength (MPa), s_f is the elongation percentage to fracture, and d is a constant value equal to 150 MPa. Caceres [21] proposed an analytical model for evaluation the variations of quality index with the microstructural features to replace the original empirical equation of quality index. This model relates the quality index value to the ductility of castings to predict material properties at different experimental situations and find the maximum value of quality index. The approximately nominal stress-strain curve is calculated using Eq 4.

$$P \cong Ks^n\exp(-s) \quad (4)$$

In Eq. 4, P and s are the stress and strain engineering value respectively, and n is the strain hardening exponent. The value of q, that is, the ductility parameter, is defined by the following equation.

$$q = \frac{s_f}{n} \quad (5)$$

Eq. 6 is obtained by replacing the q parameter in Eq.4.

$$P \cong Ks^{s/q}\exp(-s) \quad (6)$$

This equation is used in the quality index chart to generate the iso-q lines. The value of d in Eq. 1 relates to the value of K in Eq. 6 using the following equation.

$$P \cong Ks^{s/q}\exp(-s) \quad (7)$$

Finally, Eq. 8 is obtained when Eqs. 3, 4, 5 and 7 are combined.

$$Q_i = K[(qn)^n e^{-qn} + 0.4\log(100qn)] \quad (8)$$

The value of Q_i is approximated using the following equation.

$$Q_i = K[1.12 + 0.22\ln(q)] \quad (9)$$

For SEM observation tensile test specimens fracture surfaces were studied by a TESCAN electron microscopy and a LINK ISIS-Oxford energy dispersive spectroscopy (EDS) to observe the oxide films and other defects formed in the casting for finding the logical relation between the variation of casting defects and tensile test results. In addition, the melt velocity in the casting runner of different experimental cases was obtained by the SutCast software (a software for the simulation of the solidification and running system melt flow) results.

3. RESULTS

3. 1. Tensile Test Bars Results

Figs. 3 and 4 show Weibull plots for TS and %EL and, respectively, for evaluating the roll of melt filtration on tensile properties. Table 3 shows the results summary of Weibull analyses. In this table, Weibull modulus, sample numbers and regression coefficient are listed.

According to the results in Table 3, Weibull

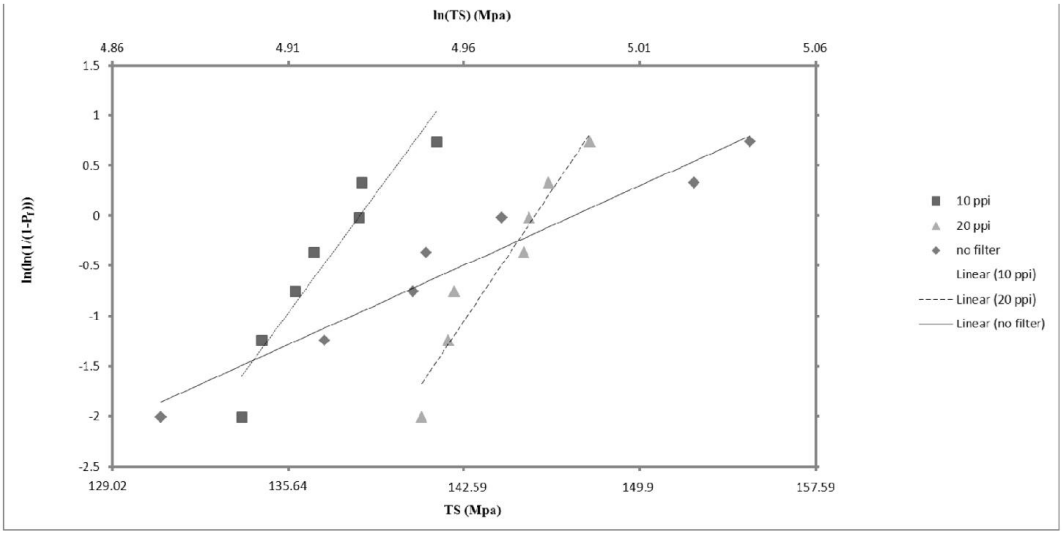

Fig. 3. Weibull plots for the tensile strength (TS) results from castings with different ceramic foam filters in the runner.

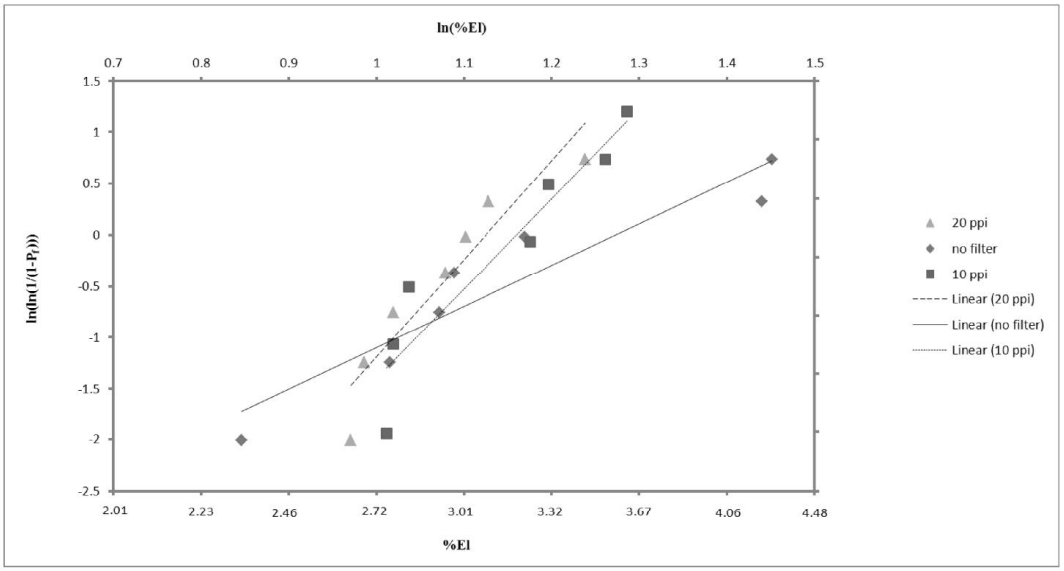

Fig. 4. Weibull plots for the %EL results from castings with different ceramic foam filters in the runner.

Table 3. Weibull modulus, sample numbers and regression coefficient of TS and %EL Weibull plots

	Filter	Sample numbers	Weibull modulus	Regression coefficient
	No filter	8	12.309	0.965
TS	10 ppi	8	28.829	0.8777
	20 ppi	8	50.397	0.9517
	No filter	8	4.0832	0.9076
%EL	10 ppi	8	6.9473	0.8985
	20 ppi	8	13.301	0.8739

modulus for TS and %EL for castings made by filters increased. Also, the Weibull modulus increased when filter with smaller pores (20 ppi) was used in the runner. This trend shows the casting made with the 20 ppi ceramic foam filter is the cleanest one.

The following equation for calculating the value of term $R^2_{0.05}$ was suggested to check whether the analyses done in the experiment is acceptable or not. Linear regression of the Weibull analyses in a study must be greater than value of $R^2_{0.05}$ [19].

$$R^2_{0.05} = \frac{1.0637 - 0.4174}{n^{0.3}} \qquad (10)$$

If the linear regression is fewer than the value of $R^2_{0.05}$, then the Weibull results are not conclusive. In this study, the term n or the number of samples for each plot was 8, so the value of $R^2_{0.05}$ was equal to 0.3463. According to Table 3, all the values of TS and %El linear regressions were higher than 0.3463, so the Weibull analyses in this study are conclusive.

Fig. 5 shows the quality index chart for different experimental cases to evaluate the effect of melt filtration on tensile strength and ductility of castings. The iso-q lines were plotted using Eq. 6 with the constant value of K equal to 200 MPa. According to this figure, test bars cast with 20 ppi ceramic foam filter (triangles) tend to follow the

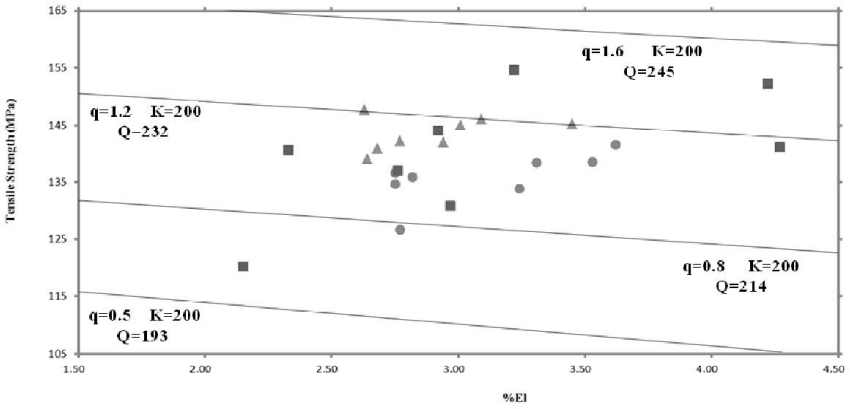

Fig. 5. The quality index chart plotted with the constant value of K equal to 200 MPa for iso-q lines. The squares, circles and triangles represent test bars cast with no, 10 ppi and 20 ppi ceramic foam filter in the runner.

line q=1.2 and Q_i=232 MPa, but other test bars (circles and squares) shift toward the lower values of q and the quality index. This trend shows the higher ductility and tensile strength in test bars cast with 20 ppi ceramic foam filter.

3. 2. SEM and EDS Results

Fractographic observation showed a considerable amount of oxide films content on the fracture surfaces of specimens that were made without using any filter in the runner. There were pores in many of these oxide films. Fig. 6(a) shows an oxide film with pores on the fracture surface of the specimen cast without using any filter. The EDS spectrum obtained from point A is shown in Fig. 7. The incoherence that weakens the alloy is exhibited in Fig. 6(b), where an example of decohesion between matrix and oxide particles is shown. The arrows in Fig. 6(b) show the path of a crack through an oxide film.

On the fracture surfaces of test bars cast using a 10 ppi ceramic foam filter, the number of observed oxide films were fewer than those made without any filters. Fig. 8(a) shows an oxide film associated with a pore in this case, and the associated X-ray spectrum from point B is also shown in Fig. 9. Also, another example of decohesion between matrix and oxide film is exhibited in Fig. 8(b). The arrows in the Fig. 8(b) indicate the route of a crack.

Few oxide films were observed on the fracture surfaces of the specimens cast with using a 20 ppi ceramic foam filter. The amount of oxide films in

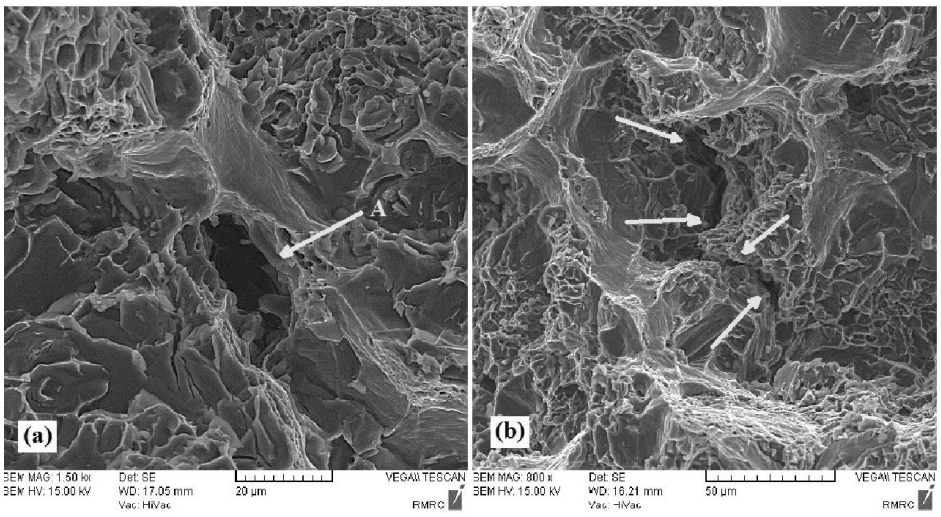

Fig. 6. Fracture surfaces of a tensile test specimen cast without any filter (a) an oxide film associated with a pore (b) the crack path among oxide particles.

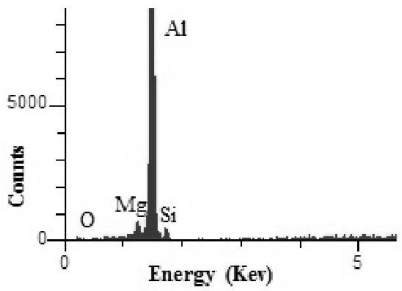

Fig. 7. The energy dispersive X-ray (EDX) spectrum from point A shown in Fig. 6(a). The spectrum corresponds to the spinel Mg . The concentration of oxygen and magnesium is equal to 4.48 wt.% and 4.88 wt. %, respectively.

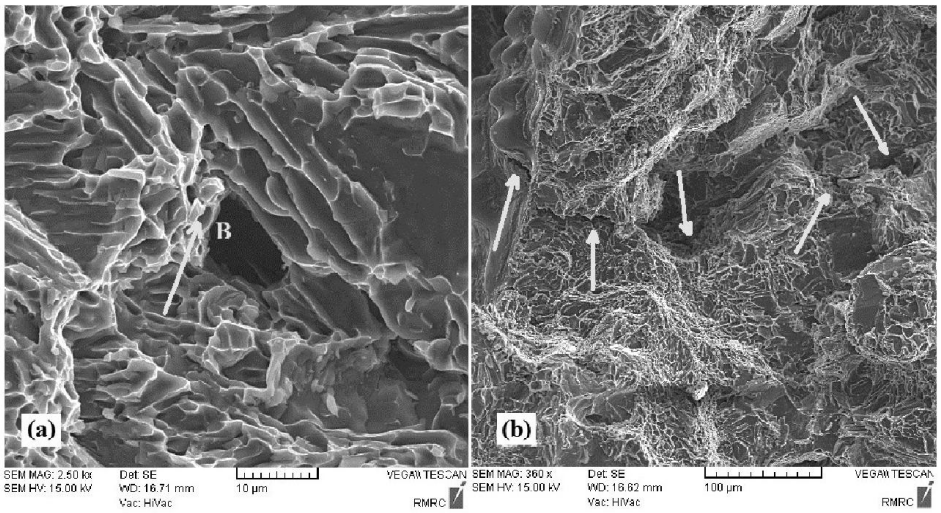

Fig. 8. Fracture surfaces of a tensile test specimen cast with a 10 ppi ceramic foam filter (a) an oxide film associated with a pore (b) the crack path among oxide particles.

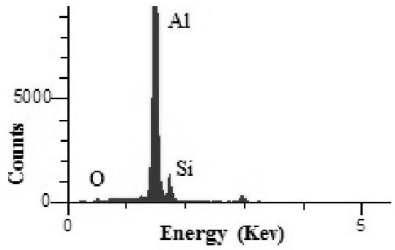

Fig. 9. The energy dispersive X-ray (EDX) spectrum from point B shown in Fig. 8(a). The spectrum corresponds to the oxide film . The concentration of oxygen is equal to 3.64 wt. %.

this experiment was fewer than the two aforementioned cases.

An interesting feature observed in the fractographic studies of the test bars cast with using a 10 ppi and 20 ppi ceramic foam filter was that there was no old oxide film on the fracture surfaces of these specimens. According to the EDS results, the maximum oxygen concentration in all oxide films observed in these two cases was 3.64 wt. %. This value indicated all of them were young oxide particles because of low concentration in oxygen peak which emanated from low thickness of young oxide films, so the melt filtration with using ceramic foam filters in this experiment was acceptable.

4. DISCUSSION

Table 3 and Figs. 3-5 show the noticeable effect of using ceramic foam filter on the tensile properties of A356 castings. According to the results of Table 3, the Weibull modulus value of the tensile strength (TS) and the percent elongation (%EL) has increased in test specimens cast with using ceramic foam filter with smaller pore size, due to the formation of fewer defects in these specimens. Also, test bars made with 20 ppi ceramic foam filter showed higher ductility and tensile strength in the quality index chart. SEM and EDS studies on the fracture surfaces of test bars revealed the formation of fewer defects in specimens cast with using ceramic foam filters with smaller pores. The deleterious effect of

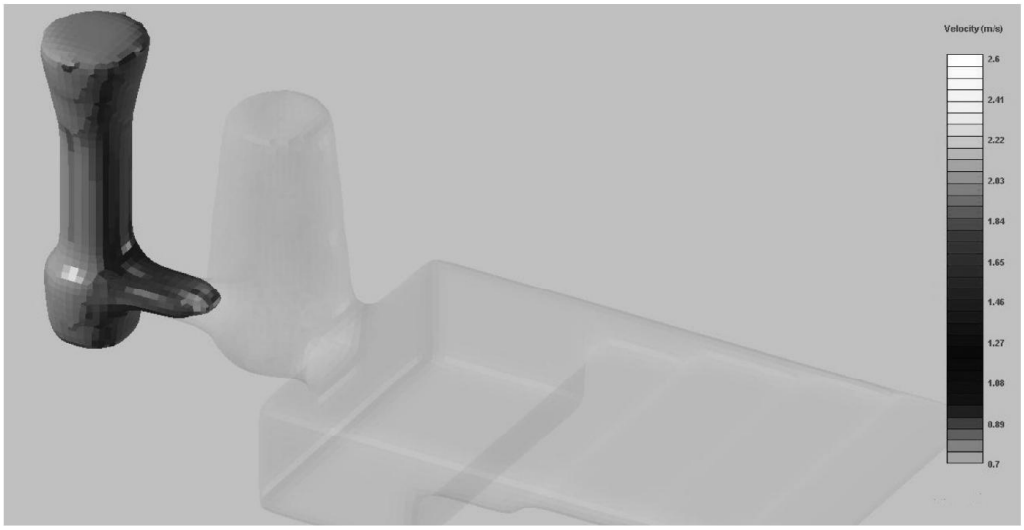

Fig. 10. The melt flow velocity in the runner of the specimen cast without any filter. (1840 mm/s)

oxide films was exhibited in the fractogaphic studies by showing the examples of decohesion between oxide films and matrix and crack path among oxide particles.

Showman [16] explained the positive roles of the ceramic foam filters in the running system. The first one is reducing the amount of oxide inclusions in the casting by preventing them from entering the mold cavity. Absence of old oxide films which are the reason for degrading tensile properties in the specimens cast with 10 and 20 ppi ceramic foam filter showed the first positive effect of using ceramic foam filters in the experiment.

The second positive effect of using ceramic filters on the tensile properties of the casting is their ability to diminish the melt flow turbulence and melt reoxidation during the mold cavity filling. Green and Campbell [2] stated that Unsuitable design of running system causes the high and undesirable melt velocity, and this leads to turbulence of melt surface, so the oxide layer at the melt surface folds and entraps in the melt. Campbell [14] showed that controlling the melt

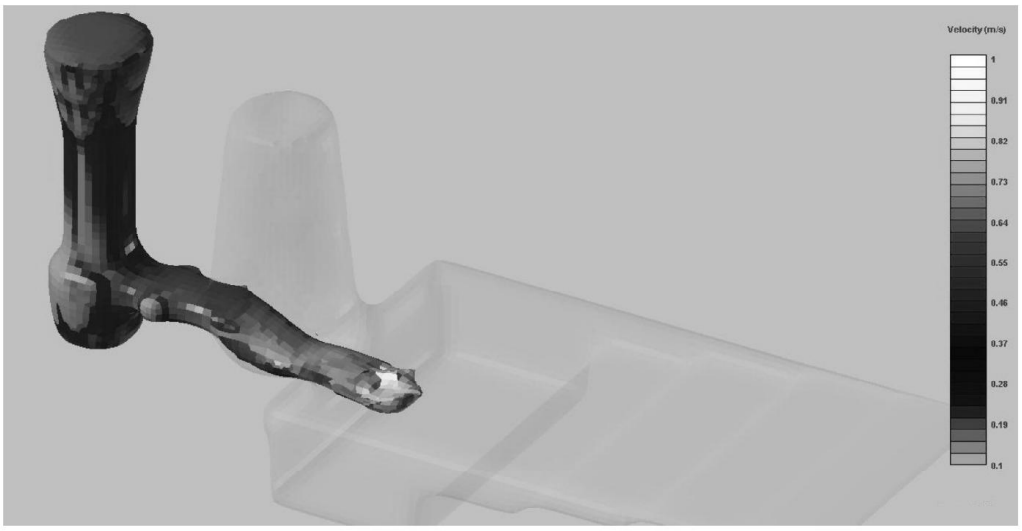

Fig. 11. The melt flow velocity in the runner of the specimen cast with a 10 ppi filter. (580 mm/s)

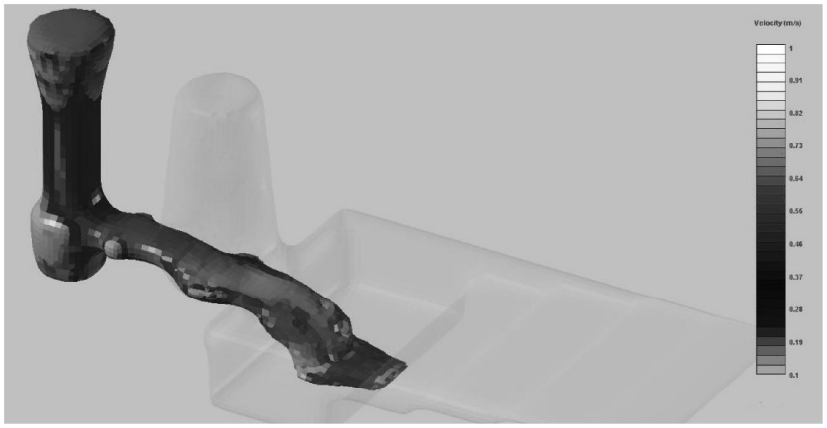

Fig. 12. The melt flow velocity in the runner of the specimen cast with a 20 ppi filter. (430 mm/s)

velocity at the range of 350 mm/s to 500 mm/s, is necessary for eliminating defects content in the casting. Figs. 10-12 shows the melt velocity in the runner after passing through the filter for casting from different experimental cases by using SutCat software results. According to the results of Figs 10-12, in the specimen cast with using a 20 ppi ceramic foam filter, the melt velocity in the runner was equal to 430 mm/s, but this value in the specimens cast with a 10 ppi ceramic foam filter and without any filter was equal to 580 mm/s and 1840 mm/s, respectively. The value of melt velocity in the specimen cast with a 20 ppi ceramic foam filter was less than critical melt velocity (500 mm/s). Therefore, fewer oxide defects and consequently higher Weibull modulus and q values were observed in these specimens.

5. CONCLUSIONS

Following conclusions could be summarized on the basis of current work:

1. Weibull modulus for TS and %EL results increases in specimens cast with using a ceramic foam filter with smaller pores.
2. The ductility parameter, q, increased in test bars cast with 20 ppi ceramic foam filter in the runner.
3. The amount of oxide films observed in the fracture surfaces of tensile test bars cast with a 10 ppi ceramic foam filter was fewer than the oxide films content in the specimens cast without any filter.
4. Few oxide films were observed on the fracture surfaces of the tensile test bars cast with a 20 ppi ceramic foam filter.
5. Absence of old oxide films in the specimens cast with 10 and 20 ppi ceramic foam filer shows one of the ceramic foam filters roles in preventing them from entering the oxide inclusions in the mold cavity.
6. By maintaining the melt flow velocity less than the critical melt velocity value (500 mm/s), ceramic foam filters decrease the amount of oxide films in the casting.

REFERENCES

1. Tiryakioğlu, M., Campbell, J., Alexopoulos, N. D., "On the Ductility of Cast Al-7%Si-Mg Alloys", Metal. Mater. Trans. A., 2009, 40A, 1000-1007.
2. Green, N., Campbell, J., "Influence of oxide film filling defects on the strength of Al-7Si-Mg alloy castings", AFS Trans., 1995, 102, 341-348.
3. Raiszadeh, R., Griffiths, W., "A method to study the history of a double oxide film defect in liquid aluminum alloys", Metall. Mater. Trans. B, 2006, 37, 865-871.
4. Ardekhani, A., Raiszadeh, R., "Removal of Double Oxide Film Defects by Ceramic Foam Filters", J. Mater. Eng. Perform., 2012, 21, 1352-1362.

5. Campbell, J., "An overview of the effects of bifilms on the structure and properties of cast alloys, Metall". Mater. Trans. B, 2006, 37, 857-863.
6. Merlin, M., Garagnani, G., "Mechanical and microstructural characterisation of A356 castings realised with full and empty cores", Metall. Sci. Tech., 2009, 27, 21-30.
7. Liu, L., Samuel, F., "Effect of inclusions on the tensile properties of Al–7% Si–0.35% Mg (A356. 2) aluminium casting alloy", J. Mater. Sci., 1998, 33, 2269-2281.
8. Yang, X., "Numerical modelling of entrainment of oxide film defects in filling of aluminium alloy castings", Inter. J. Cast Metal. Res., 2004, 17, 321-331.
9. Campbell, J., Castings, Butterworth Heinemann, Oxford, 1991.
10. Cao, X., Campbell, J., "Effect of Precipitation of Primary Intermetallic Compounds on Tensile Properties of Cast Al - 11.5 Si - 0.4 Mg Alloy", AFS Trans., 2000, 108, 391-400.
11. Campbell, J., Divandari, M., "Mechanisms of Bubble Trail Formation in Castings", AFS Trans., 2001, 109, 433-442.
12. Halvaee, A., Campbell, J., "Critical Mold Entry Velocity for Aluminum Bronze Castings", AFS Trans., 1997, 105, 35-46.
13. Runyoro, J., Boutorabi, S., Campbell, J., "Critical Gate Velocity for Film-Forming Casting Alloys"; Abasic for Process Specification, Chuk., 1997, 23, 67-77.
14. Campbell, J., "Invisible macrodefects in castings", J. Phys. IV, 1993, 3, 7-7.
15. Cáceres, C. H., Selling, B. I., "Casting defects and the tensile properties of an AlSiMg alloy", Mater. Sci. Eng. A, 1996,220, 109-116.
16. Showman, R. E., "Choosing the best ceramic filter to improve Aluminium casting properties", AFS Trans., 2007, 115, 199-206.
17. Habibollah Zadeh, A., Campbell, J., "Metal flow through a filter system", AFS Trans., 2002, 110, 1-17.
18. Hashemi, H., Raiszadeh, R., "Naturally-pressurized system. The role of ceramic filters", J.appl. sci, 2009, 9, 2115-2122.
19. Tiryakioğlu, M., Hudak, D., Ökten, G., "On Evaluating Weibull Fits to Mechanical Testing Data", Mater. Sci. Eng. A, 2009, 527, 397-399.
20. Drouzy, M., Jacob, S., Richard M., "Interpretation of tensile results by means of quality index and probable yield strength", AFS Int. Cast Metals Jnl., 1980, 5, 43-50.
21. Cáceres, C.H., "A rationale for the quality index of Al-Si-Mg casting alloys", Int. J. Cast Metals Res., 1998, 10, 293-299.